The Mechanics of Geometric Stripping

Augusto E. Barton, Xerox Corporation, Webster, NY

Abstract

The paper describes a dynamic model for a toner-laden sheet being bent on a rotating fusing surface with a radius. The toner is treated as visco-elastic, with a complex modulus that is a function of temperature and frequency. Other inputs include toner thickness, media modulus, and media thickness. The model can quantify the contribution of the following to successful stripping: stripping radius, process speed, toner rheological properties, toner temperature, toner thickness, and media stiffness. The model can also be used to predict the impact of more complicated scenarios, like varying image/paper bleed dimensions and external stripping devices.

Motivation

The release of toner-laden media from a fuser, commonly referred to as stripping, is a function required by all fusers. Self-stripping, a condition in which no external forces are required, is highly desired, as it avoids the use of stripper fingers that wear the fusing surface or an air knife that can cause differential cooling.

We present here a geometric stripping model that calculates the stripping stresses induced in the toner-fuser interface as a sheet with visco-elastic toner is bent on a fusing surface with a radius. A geometric stripping model of this type, which includes toner mechanical properties, permits one to not only design a fuser capable of stripping a given toner but to also define the stripping requirements for a given toner. Thus this modeling technique permits one to view stripping as a system-level optimization of fuser design and toner materials.

Geometric stripping model

Paper is modeled as a thin plate under a load distribution. The model considers that a portion of the paper length is conformed to the radius and the remainder is not, producing a length of the paper to be under toner strain being that called the under-strain-length L_{us}. Toner is modeled as a visco-elastic material attached to both the paper and the radius. As the radius rotates, the paper bends, pulled to the radius by the toner under tension. The toner layer's dynamic stress and strain depend on the paper dynamic loading as well as the toner complex stiffness. This is calculated by using a discrete model which calculates for each time step the toner stress and strain, which is a result of the mechanical interaction between the toner and paper as well as the state of previous time steps. The model calculates the stress level in the toner-fuser interface as a function of time, assuming that the toner does not separate from the rotating fusing surface radius, to calculate maximum stress and determine if stripping will occur.

Paper bending on a radius – model

For a beam or thin plate with a distributed load bending on a radius, there is a given moment M at which its radius of curvature ρ equals the radius R and so starts touching the radius. As shown by Timoshenko [1], a cantilevered thin plate under load has a radius of curvature $\rho = M/(2D)$ at the cantilevered end A. If the plate is tangent to a radius R at the same point A then from the equation

$$M_{limit} = \frac{2D}{R} \tag{1}$$

we can obtain the limiting moment M_{limit} at which the plate starts becoming in contact with the radius beyond the point A.

For the particular case in which the paper is bent over a radius due to the load induced by a toner layer under tension then the paper will only be subjected to a load in the length at which the toner is stretched which is called the under-strain-length L_{us}.

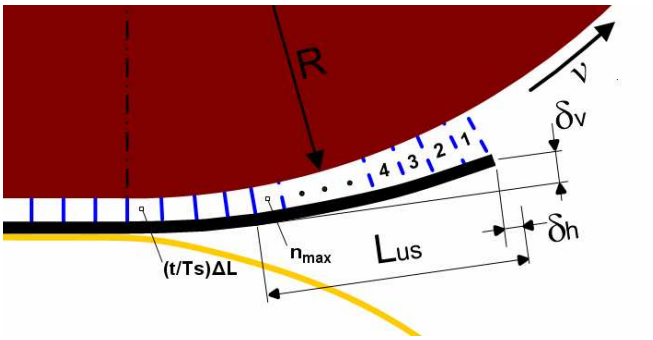

Figure 1. *Schematic of Geometric Stripping Discrete Model*

The paper deflection is calculated using the moment area method as described by Timoshenko et al. [2]. The vertical deflection at the tip of the paper δ_v is calculated as a function of the moment distribution M_i which is a function of the load distribution q_i equal to the toner stress distribution σ_i (due to the model assuming a unit paper width) and the moment at the tip called M_1 as shown in Eq. 2.

$$\delta_v[n] = \frac{\Delta L^2}{2D} \sum_{j=1}^{n\max[n]} (M_j[n] + M_{j+1}[n])(j - 1/2)$$
$$M_i[n] = \Delta L^2 \sum_{j=1}^{i-1} \sigma_j[n](i - j - 1/2) + M_1[n] \tag{2}$$

where ΔL: element length, D: bending stiffness, n_{max}: number of under-strain elements, n: model step. The model step n relates to the simulated time t as defined by $t=(n\text{-}1)T_s$, where T_s is the model time step. The element length ΔL relates to the time step T_s and the process speed v by $\Delta L = T_s\, v$. The number of under-strain elements $n_{max}=L_{us} / \Delta L$ is calculated each iteration step by checking the location n_1 at which it's corresponding moment M_1 exceeds the

limiting moment M_{limit} (from Eq. 1) is exceeded, and so the number of under-strain elements $n_{max}=n_1 - 1$.

Similarly the horizontal deflection at the tip of the paper δ_h is calculated adding up the horizontal deflection of each element due to their angle calculated using the moment area method described by Timoshenko et al. [2] as shown in Eq. 3.

$$\delta_h[n]=\Delta L\sum_{j=1}^{n\max[n]}\left(1-\cos\left(\theta_{j+1}[n]\right)\right)$$
$$\theta_i[n]=\frac{\Delta L}{2D}\sum_{j=i}^{n\max[n]}\left(M_j[n]+M_{j+1}[n]\right) \quad (3)$$

Based on the paper deflection the gap between the paper and the radius at the lead edge of the toner is calculated using Eq. 4.

$$gap_{tip}[n]=\left[\left(L_{us}[n]-\delta_h[n]\right)^2+\left(R-\delta_v[n]\right)^2\right]^{1/2}-R \quad (4)$$

Mechanical interaction between toner and paper

While the paper advances and bends on the rotating fusing surface radius the toner is subjected to normal strain within the under-strain length $L_{us}=(n_{max}-1)\Delta L$, with that strain being a maximum at the lead edge of the image and zero at the point were the paper is conformed to the radius. The normal strain distribution is defined by Eq. 5 which assumes the strain distribution grows from zero to $\varepsilon_{toner,i=1}$ proportional to the fourth power of the under-strain length.

$$\varepsilon_i[n]=\frac{\left(\varepsilon_{toner,\,i=1}\right)}{n_{\max}[n]^4}\left(n_{\max}[n]-i+1\right)^4 \quad ,i\geq 2 \quad (5)$$

The toner stress distribution q_i is calculated for every model step based on the history of its stress distribution q_i and strain distribution ε_i and its complex modulus, using a standard difference equation (Eq. 6) as defined by Oppenheim et al. [3].

$$\varepsilon_i[n]=\frac{1}{a_0}\left\{\sum_{k=0}^{M}b_k\sigma_i[n-k]-\sum_{k=1}^{N}a_k\varepsilon_i[n-k]\right\} \quad (6)$$

where a_0, a_k and b_k are difference equation coefficients, and M and N are the feedforward and feedback order respectively, defined by the inverse of the toner complex modulus in z-transform form as shown in Eq. 7.

$$\frac{\mathrm{E}(z)}{\Sigma(z)}=\frac{b_0+b_1z^{-1}+\cdots+b_Mz^{-M}}{1+a_1z^{-1}+\cdots+a_Nz^{-N}},$$
$$\mathrm{E}(z)\overset{Z}{\leftrightarrow}\varepsilon[n],\quad \Sigma(z)\overset{Z}{\leftrightarrow}\sigma[n] \quad (7)$$

At each time step n the model iterates so that the stress distribution q_i yields a paper deflection such that the gap at the lead edge of the toner equals the toner thickness extension as defined by Eq. 8.

$$gap_{tip}=\left(\varepsilon_{toner,\,i=1}\right)\cdot t_{toner} \quad (8)$$

Toner complex modulus model

The toner is modeled as visco-elastic with a complex shear modulus that is frequency and temperature dependent. For standard electrophotographic toners, the complex modulus increases with frequency and decreases with temperature. The toner complex shear modulus is $G=G'+jG''$, where G' and G'' are known as the storage shear modulus and the loss shear modulus. The complex shear modulus G has a magnitude $|G|=(G'^2+G''^2)^{1/2}$ and phase $\varphi=\tan^{-1}(G'/G'')$. We have considered two types of models for the toner complex modulus G, both in the Laplace domain where $s=j\omega$. The first is a generalized Maxwell model based on the representation by Jones [4], shown in Eq. 9. The second is a transfer function with multiple poles and zeros, shown in Eq. 10. The author prefers the use of the pole zero method since it is more direct.

$$G(s)=G_0+\frac{G_1\eta_1 s}{G_1+\eta_1 s}+\frac{G_2\eta_2 s}{G_2+\eta_2 s}+\cdots+\frac{G_n\eta_n s}{G_n+\eta_n s} \quad (9)$$

$$G(s)=G_0\frac{(s/\omega_1+1)(s/\omega_3+1)\cdots(s/\omega_{n-1}+1)}{(s/\omega_2+1)(s/\omega_4+1)\cdots(s/\omega_n+1)} \quad (10)$$

The temperature effect on the toner complex modulus was modeled using a shift factor $a_T=f(T_{toner},T_0)$ as explained by Ferry [5], where T_{toner} is the temperature of interest and T_0 is the reference temperature at which the toner complex modulus was measured or the reference temperature used to create the complex modulus master curve. The complex modulus can then be calculated for any operating temperature T_{toner} using the following transformation $G_T(\omega)=G_{To}(\omega a_T)$. Note Ferry [5] also makes a correction for the thermal expansion of the viscoelastic material by using a factor $T\rho/T_0\rho_0$ to affect the modulus, but the effect of that factor is small and is not considered in the present analysis.

The Laplace form of the shear complex modulus as a function of temperature can be found by replacing $s=j\omega$ with $sa_T=j\omega a_T$ in Eq. 10:

$$G_T(s)=G_0\frac{(sa_T/\omega_1+1)(sa_T/\omega_3+1)\cdots(sa_T/\omega_{n-1}+1)}{(sa_T/\omega_2+1)(sa_T/\omega_4+1)\cdots(sa_T/\omega_n+1)} \quad (11)$$

Based on Eq. 11 the toner compliance can be calculated as shown in Eq. 12. The toner compliance z-transform transfer function from Eq. 7 can be obtained by finding the z-transform equivalent to the Laplace transfer function from Eq. 12. This was found using the MATLAB® [6] c2d function which discretizes the continuous-time linear time invariant model using zero-order hold on the inputs and the model time step T_s.

$$\frac{\mathrm{E}(s)}{\Sigma(s)}=\frac{1}{3G(s)}\xrightarrow{\text{L to Z}}\frac{\mathrm{E}(z)}{\Sigma(z)}=\frac{b_0+b_1z^{-1}+\cdots+b_Mz^{-M}}{1+a_1z^{-1}+\cdots+a_Nz^{-N}} \quad (12)$$

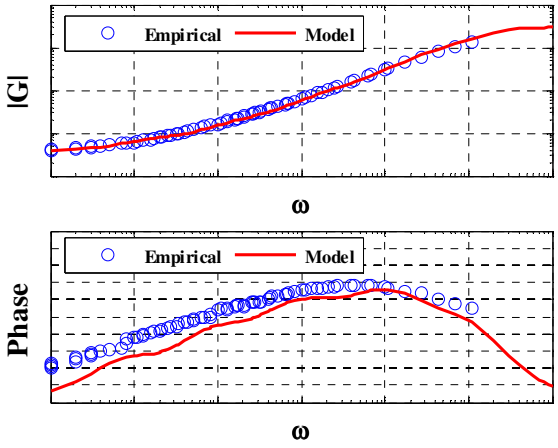

Figure 2. *Toner complex modulus model fit to empirical data*

Fit to empirical data

The toner complex modulus, obtained from rheological measurements, can be modeled by fitting Eq. 10 as shown in Fig. 2. This was done by first defining the complex modulus G_0, which is the complex modulus at low frequencies defined by the low frequency complex modulus plateau. Following the definition of G_0, the pole and zero pairs were defined to fit the empirical toner complex modulus and phase. The more pole and zero pairs used the better model fit that can be achieved. The toner complex modulus fit shown in Fig.2 was obtained by using 7 pole and zero pairs.

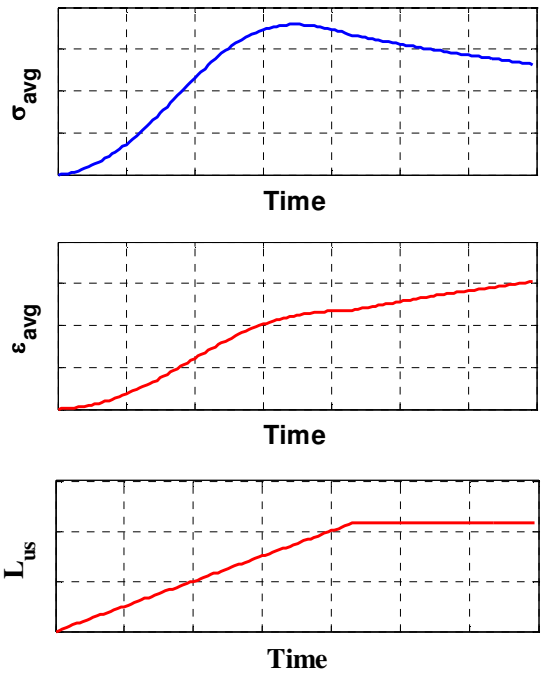

Figure 3. *Typical simulation results from stripping model*

Simulation results

As explained earlier the model assumes that the toner stress and strain can rise without bounds. The model makes that assumption in order to quantify the maximum possible toner stress that can be reached at given stripping conditions. That permits one to quantify the effect of different stripping inputs on peak stress and define the required level of stress for stripping to occur by correlating the model with empirical results. The peak stress required for stripping can then be linked to the maximum sustainable toner-fuser interface stress. Note this stress is often modulated by release agents applied to the fuser surface (e.g., standard silicone oils) or by release agents embedded within the toner (e.g., standard polyester or polypropylene waxes).

The maximum sustainable stress is not a fixed value, since it has been proven empirically that it is dependent on details of the fusing surface, the release agent, and the toner. The maximum sustainable stress was back-calculated from stripping tests with media and toner of known mechanical properties to estimate the level at which stripping is imminent. An attempt was made also to measure the maximum allowable release-agent stress empirically but the available test equipment was unable to replicate the complex conditions to which the toner-fuser interface is exposed during the stripping process. For that reason the author has found the former method more effective in calculating the maximum sustainable interface stress.

In Fig. 3, the model clearly shows how the toner stress grows until reaching a peak, while the toner strain increases monotonically. This results indicate that in the case where the peak stress does not exceed the maximum sustainable stress, the toner strain could increase to a level at which the toner could potentially split. Also the under-strain length L_{us} increases with time and reaches a maximum as shown in Fig. 3. For that reason an inflection in both the toner stress and strain can be observed at the time at which the under-strain length reaches a maximum.

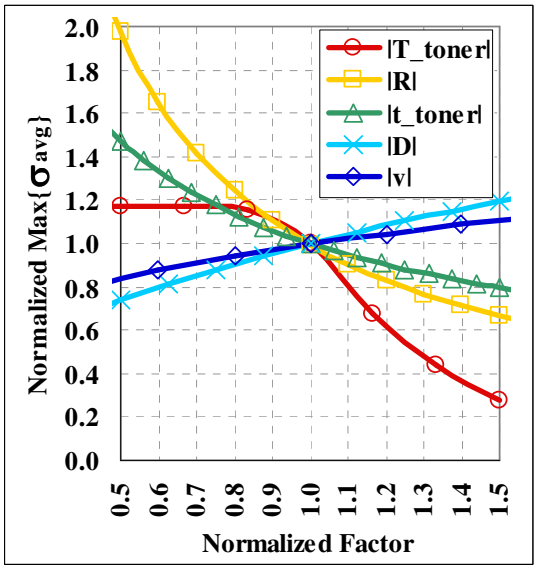

Figure 4. *Effect of individual factors on Max average toner stress*

Effect of individual stripping model inputs

The effect of the individual stripping model inputs was analyzed by choosing a nominal value for all the inputs and using its corresponding maximum average stress as reference. The result of that analysis is summarized in Fig. 4. The factors that drove stripping were, in rough order of importance:

- Toner temperature T_{toner}. Reduces the stress dramatically at elevated temperature, but does not increase the stress below a certain temperature. When the toner temperature increases its complex modulus shifts to higher frequencies and so becomes more compliant and reduces the paper bending as well as the toner stress.
- Stripping radius R. By making the stripping radius smaller the paper will bend around the radius at a higher rate as well as induce higher paper bending moment and so induce a higher toner stress due to the higher toner complex stiffness at higher rates (which is analogous to higher frequencies).
- Toner thickness t_{toner}. A thicker toner pile will increase its compliance and so reduce the paper bending as well as the toner stress.
- Paper bending stiffness D. Toner stress increases with paper bending stiffness due to higher loads required to bend the paper around the radius.

– Process speeds *v*. Higher process speeds will increase toner stress since both the paper will bend and the toner will strain at a higher rate. At these rates, the toner has higher complex stiffness and as a consequence results in higher toner stress.

Conclusions

A model has been developed that quantifies the stresses to which a toner-fuser interface is subjected as a toner-laden sheet is run against a radius. This model enables one to quantify the effect of the toner complex modulus, temperature, toner thickness, stripping radius, paper bending stiffness, and process speed. It can be easily upgraded to include the effects of more complicated interactions, such as the effect of lead edge bleed with paper weight, as well as with external stripping mechanisms such as an air knife.

The model has been validated experimentally, and shows several interesting results. Avoiding excessive fusing temperature will increase the stripping latitude dramatically. This is due to the fact that the reduction of toner stiffness is limited, and as a consequence the reduction of max toner stress is limited as well. The stripping radius is the main fuser-design factor that has substantial effect on stripping. The toner max stress is directly proportional to *1/R* which means halving the radius will double the maximum stress induced on the toner.

The model can be used in combination with empirically derived stripping latitude to define stripping radius requirements in combination with other design-limiting factors. The stripping model can also quantify the effect of toner thickness on stripping latitude when increasing toner mass per area and hence toner thickness.

Acknowledgements

The author wants to thank A. Schnuerch for multiple toner rheology measurements, J. Padula for his collaboration on the experimentation, and D. Bott for the technical editing of this paper.

References

[1] S. Timoshenko, *Strength of Materials, Part II, Advanced Theory and Problems (Third Edition).* Robert E. Krieger, Malabar, FLA, 1983, pg.69-70.

[2] S. Timoshenko, and J. Gere. *Mechanics of Materials*. D. Van Nostrand Company, New York, 1972; pg. 176-181.

[3] A. Oppenheim, and A. Willsky. *Signals and Systems (Second Edition).* Prentice Hall, NJ, 1997, pg. 121-124.

[4] David I. G. Jones. *Viscoelastic Vibration Damping*. Wiley, 1992.

[5] John D. Ferry. *Viscoelastic Properties of Polymers (Third Edition).* John Wiley & Sons, Inc., NY, 1980, pg. 264-280

[6] MATLAB version 7.4.0.287, Natick, Massachusets: The Mathworks Inc., 2007.

Author Biography

Augusto Barton joined Xerox in 2005 and currently works in the Xerox Innovation Group. Since 2005, he worked on various research initiatives in Xerographic related areas, particularly in fusing. His research interests include fusing systems and subsystems, controls, numerical analysis, finite elements, and precision machine design. Augusto received his BSc in Mechanical Engineering (1999), from the Pontifical Catholic University of Peru, and received a MSc. in Mechanical Engineering (2005), from the Massachusetts Institute of Technology.